J Membrane Biol (2009) 230:143–154
DOI 10.1007/s00232-009-9195-z

EtpB Is a Pore-Forming Outer Membrane Protein Showing TpsB Protein Features Involved in the Two-Partner Secretion System

Albano C. Meli · Maria Kondratova · Virginie Molle · Laurent Coquet · Andrey V. Kajava · Nathalie Saint

Received: 4 May 2009 / Accepted: 28 July 2009 / Published online: 27 August 2009

Abstract Attachment to host tissues is a critical step in the pathogenesis of most bacterial infections. Enterotoxigenic *Escherichia coli* (ETEC) remains one of the principal causes of infectious diarrhea in humans. The recent identification of additional ETEC surface molecules suggests that new targets may be exploited in vaccine development. The EtpA protein identified in ETEC H10407 is a large glycosylated adhesin secreted via the two-partner secretion system. EtpA requires its putative partner EtpB for translocation across the outer membrane (OM). We investigated the biochemical and electrophysiological properties of purified EtpB. We showed that EtpB is 65-kDa heat-modifiable protein localized to the OM. Electrophysiological experiments indicated that EtpB is able to form pores in planar lipid bilayer membranes with an asymmetric current, suggesting its functional asymmetry. The pore of EtpB frequently assumes an opened conformation and fluctuates between three well-defined conductance states. In silico analysis of the EtpB amino acid sequence and molecular modeling suggest that EtpB is similar to the well-known TpsB protein FhaC from *Bordetella pertussis* and has a C-terminal transmembrane β-barrel domain that is occluded by an N-terminal α-helix, an extracellular loop, and two periplasmic polypeptide-transport-associated (POTRA) domains. Together, these data confirm that EtpB is a pore-forming protein mainly folded into a β-barrel conformation and indicate that EtpB presents typical features of the OM TpsB proteins.

Keywords Type V secretion · ETEC · Transporter · Channel activity · Molecular modeling

A. C. Meli · N. Saint (✉)
Centre de Biochimie Structurale, CNRS UMR 5048, Université Montpellier 1 et 2, 34090 Montpellier, France
e-mail: nathalie.saint@inserm.fr

A. C. Meli · N. Saint
INSERM U554, 34090 Montpellier, France

M. Kondratova · A. V. Kajava
Centre de Recherches de Biochimie Macromoleculaire, CNRS UMR 5237, Université Montpellier 1 et 2, 34293 Montpellier cedex 5, France

V. Molle
Institut de Biologie et de Chimie des Protéines, Université de Lyon, CNRS UMR 5086, 69367 Lyon, France

L. Coquet
UMR 6522 CNRS, PBM, Plate-forme Protéomique IFRMP23, Université de Rouen, 76821 Mont-Saint-Aignan, France

Introduction

The transport of proteins across membranes to their final destination in the cell is an essential function of all living organisms. Secretion of enzymes, adhesins and toxins to the cell surface or into the extracellular milieu is an important component of bacterial pathogenesis. Gram-negative bacteria have a complex cell envelope composed of two distinct membranes, the cytoplasmic and outer membranes (OM), and have developed specific mechanisms to translocate proteins through the cell envelope (Cascales and Christie 2003; Desvaux et al. 2004; Holland 2004; Kostakioti et al. 2005; Mota et al. 2005; Pukatzki et al. 2006; Thanassi et al. 2005). Many essential virulence factors are secreted via the type V two-partner secretion (TPS) system which is considered to be the simplest of the six known protein secretion mechanisms (Henderson et al.

1998; Jacob-Dubuisson et al. 2001; Mougous et al. 2007; Schell et al. 2007). The TPS system is composed of a large exoprotein (TpsA) secreted by its specific cognate transporter partner (TpsB). Despite the fact that the two partners are translated as two separate proteins, they are typically encoded in the same operon or in the same genomic locus (Jacob-Dubuisson et al. 2001).

TPS family TpsA/TpsB pairs that have been functionally characterized include FHA/FhaC of *Bordetella pertussis,* ShlA/ShlB of *Serratia marcescens*, and HMW1/HMW1B of *Haemophilus influenzae* (Guedin et al. 2000; Konninger et al. 1999; St Geme and Grass 1998). TpsA protein sequences are variable, although they have three common features: they are large (many $>$ 3,000 aa and some $>$ 5,000 aa), they share significant sequence similarity within their N-terminal 300 aa (a region called the TPS domain), and most contain stretches of repeated sequences that are predicted to form β-helical or β-solenoid structures (Junker et al. 2006; Kajava et al. 2001; Kajava and Steven 2006). The crystal structures of both Fha30 and HMW1 pro-piece revealed that the TPS domain folds into a β-helix (Clantin et al. 2004; Yeo et al. 2007). By contrast, the TpsB proteins belong to the Omp85/TpsB superfamily of protein-translocating OM porins. This superfamily contains members in the animal, plant and fungal kingdoms, making this the most distributed general secretion mechanism in nature (Yen et al. 2002). TpsB proteins are typically $\sim$500–800 aa and are highly conserved. The TpsB proteins contain common features including a C-terminal transmembrane β-barrel and one to five polypeptide transport associated (POTRA) N-terminal domains which are known to be essential for interactions with TpsA partners (Sanchez-Pulido et al. 2003). TpsB proteins have at least two distinct functions. First, the TpsB protein must recognize and interact with the secretion domain of the TpsA periplasmic intermediate. Second, the TpsB protein must form a pore to allow the secretion of the TpsA protein. It has been shown that TpsB proteins form pores with diameters of 1–3 nm (Duret et al. 2008; Jacob-Dubuisson et al. 1999; Konninger et al. 1999; Surana et al. 2004). Recently, a 3.15 Å crystal structure of FhaC has been solved, providing new insight into the organization of TpsB proteins. The FhaC transporter comprises a 16-stranded β-barrel that is occluded by an N-terminal α-helix and an extracellular loop L6, along with a periplasmic module composed of two aligned POTRA domains (Clantin et al. 2007). Pore-forming activity studies of FhaC have indicated a conductance of 1,200 pS in 1 M KCl (Jacob-Dubuisson et al. 1999; Meli et al. 2006). Although deletion of the POTRA domains abrogated secretion, channel activity persisted in the absence of the periplasmic module (Clantin et al. 2007; Meli et al. 2006). Interestingly, deletion of L6 also abolished secretion, modified the channel activity and reduced the ionic conductance even though the pore size increased (Clantin et al. 2007). On the basis of the FhaC structure and functional experiments, Clantin and colleagues proposed a model of FHA transport whereby the N-terminal TPS domain of FHA initially interacts in an extended conformation with the FhaC POTRA 1 domain in the periplasm, given the orientation of the POTRA domains relative to the channel. The FHA-FhaC interactions would then bring the region corresponding to the first repeats of the central β-helical domain of FHA in proximity to the tip of loop L6. Conformational changes in FhaC would then expel loop L6 out of the β-barrel, thus opening a larger channel for FHA translocation (Clantin et al. 2007). General features of the mechanism obtained here are likely to apply throughout the superfamily (Jacob-Dubuisson et al. 2009; Knowles et al. 2009).

The enterotoxigenic *Escherichia coli* (ETEC) are a diverse group of pathogens that cause infectious diarrhea after the ingestion of contaminated food and water. ETEC are responsible for considerable morbidity in developing countries and are an emerging cause of diarrheal illness in several recent large-scale outbreaks in the United States (Beatty et al. 2004, 2006; Daniels 2006; Roels et al. 1998). In 2006, Fleckenstein and colleagues suggested the presence of a TPS in ETEC, which they named *etpBAC* on the basis of the nomenclature used for homologous loci, including the *Yersinia enterocolitica rscBAC* locus and the prototype *H. influenzae hmwABC* locus (Barenkamp and St Geme 1994; Fleckenstein et al. 2006; Nelson et al. 2001). The homology of the proteins encoded at this locus to known TpsA and TpsB proteins predicts that the secretion of EtpA exoprotein (TpsA) requires both EtpC and EtpB. EtpC is a glycosylase that shares homology with RscC and HMW1C proteins and the EtpB protein is predicted to be an OM transporter (TpsB). Recently the large glycosylated EtpA protein was shown to contribute to colonization of the intestine and to act as a protective immunogen in an experimental mouse model (Roy et al. 2008). Moreover interactions between EtpA and flagella have been demonstrated to be critical for adherence and intestinal colonization (Roy et al. 2009).

In this work, we have characterized the biochemical and electrophysiological properties of EtpB protein which is the putative TpsB transporter of ETEC. We also performed in silico sequence analysis and molecular modeling of EtpB and demonstrated its similarity to the recent X-ray structure of FhaC, a typical representative member of the Omp85-TpsB superfamily. Together, these results establish that EtpB is an OM TpsB member. They are also consistent with the hypothesis that EtpB is the TpsB partner involved in the secretion of the EtpA adhesin of ETEC.

Methods

Cloning, Expression, and Purification of Recombinant EtpB

A 1737-bp *etpB* gene fragment lacking the putative signal sequence was amplified by PCR from pJMF1002 (provided by James Fleckenstein's laboratory, University of Tennessee Health Science Center, Memphis, TN) (Fleckenstein et al. 2006), using primers #353, 5′-TAT *GGA TCC* GCT TCA AAA GCA GGT GAG CAC GGC CGC CTC TCC GTT CCG-3′ (containing a *Bam*HI site indicated in italic and five linker codons indicated by underlining), and primer #354, 5′-TAT *AAG CTT* TTA GAA CGT TTT CAG GGC TGA CAG-3′ (containing a *Hin*dIII site indicated in italic). The PCR product was digested with *Bam*HI and *Hin*dIII and ligated into the pETSIGL vector prepared by previous digestion with the same enzymes, yielding pETSIGL_*etpB*. The pETSIGL vector is a pETSIG (Siroy et al. 2005) derivative that enables production of the His-tagged protein of interest as an N-terminal fusion product with the signal peptide of *E. coli* OmpA porin allowing targeting of the proteins to the OM. A thrombin cleavage site is added between the His-tag and the protein to eliminate the tag after purification.

Escherichia coli BL21(DE3)*omp8* cells were transformed with pETSIGL-*etpB* (Prilipov et al. 1998). The recombinant strains were selected on LB agar supplemented with carbenicillin and kanamycin. Liquid cultures were incubated at 37°C with shaking until an A_{600} (absorbance at 600 nm) of 0.6 was reached. The expression of the recombinant gene was then induced by the addition of isopropyl-1-thio-β-D-galactoside (IPTG) at a final concentration of 0.5 mM, after which the bacteria were grown in the same conditions for 3 h. Cells were collected by centrifugation for 10 min at 6,000*g* and resuspended in a lysis buffer [150 mM sodium chloride (NaCl) 20 mM sodium phosphate (NaPi) (pH 7.2), 5 mg of Complete ETDA-free antiprotease cocktail (Roche Applied Science, Basel, Switzerland), 10% glycerol, 1 mM mercaptoethanol, 0.01 mg/ml DNAse, and 0.01 mg/ml lysozyme]. The bacteria were then disrupted by sonication and the resulting suspension was centrifuged for 1 h at 55,000*g* at 4°C. The membrane pellet was resuspended and incubated at 37°C for 1 h in a buffer [150 mM NaCl 20 mM NaPi (pH 7.2), 2% *n*-octyl-polyoxyethylene (OPOE, Bachem), 5 mg 4-(2-aminoethyl) benzenesulfonyl fluoride hydrochloride (AEBSF) (Roche Applied Science). The final suspension was centrifuged at 55,000*g* for 1 h at 4°C.

For purification of the His tagged EtpB proteins, the supernatants were incubated with Ni-NTA (Ni^{2+}-nitrilotriacetate)-agarose suspension (Qiagen, Hilden, Germany). The protein–resin complex was packed into a column and washed extensively with a buffer consisting of 150 mM NaCl 20 mM NaPi (pH 7.2), 10 mM imidazole and 1% OPOE. The proteins were eluted with the same buffer in the presence of 400 mM imidazole.

The protein solutions were concentrated with a spin concentrator (Centricon, cutoff 10 kDa, Amicon) before being loaded onto a gel filtration column (Superdex 75, GE Healthcare). The elution buffer consisted of 300 mM NaCl 20 mM NaPi (pH 7.2) and 1% OPOE. The eluted fractions were analyzed by 12% sodium dodecyl sulfate–polyacrylamide gel electrophoresis (SDS-PAGE) and visualized by Coomassie blue staining. Protein concentrations were determined by measuring the absorbance at 280 nm (Nanodrop; Labtech).

SDS-PAGE and Mass Spectrometry Analysis

The OM protein samples containing the recombinant EtpB proteins were analyzed by SDS-PAGE with a 4% polyacrylamide stacking gel (pH 6.8), a 12% polyacrylamide resolving gel (pH 8.8) and stained with Coomassie brilliant blue G. Samples containing the purified recombinant EtpB were analyzed by western blot with a rabbit polyclonal anti-EtpB antibody generously provided by James Fleckenstein's laboratory. The immunoblots were revealed using a goat alkaline phosphatase-conjugated secondary antibody from Pierce.

For protein identification by mass spectrometry, protein bands from the SDS-PAGE gels with an apparent molecular mass of approximately 65 kDa were cut with a scalpel. Excised fragments were washed several times and dried for a few minutes. Trypsin digestion was performed overnight with a dedicated automated system (MultiPROBE II, PerkinElmer). The gel fragments were subsequently incubated twice for 15 min in a H_2O/CH_3CN solution to allow extraction of peptides from the gel pieces. Peptide extracts were then dried and solubilized in starting buffer for chromatographic elution, consisting of 3% CH_3CN and 0.1% HCOOH in water. Peptides were enriched and separated with lab-on-a-chip technology (Agilent) and fragmented with an online XCT mass spectrometer (Agilent). The fragmentation data were interpreted by the DataAnalysis program (version 3.4, Bruker Daltonic).

The tandem mass spectrometry peak lists were extracted and compared with the NCBInr protein database by the Mascot Daemon (version 2.2.2) search engine. All searches were performed with no fixed modification and with variable modifications for carbamidomethylation of cysteines, for oxidation of methionines, and with a maximum of one missed cleavage. Tandem mass spectrometry spectra were searched with a mass tolerance of 1.2 Da for precursor ions (MS data) and 0.6 Da for fragment ions (MS2 data). The protein identification was validated if at least two peptides

exhibited individual ions scores higher than the average default value for significance by Mascot.

Planar Lipid Bilayer Recordings

Virtually solvent-free planar lipid bilayers were formed over a 125–200-μm hole in a polytetrafluoroethylene film (10 μm thick) pretreated with a mixture of 1:40 (v/v) hexadecane/hexane and sandwiched between two half glass cells as described (Meli et al. 2006). Phosphatidylcholine from soy beans (azolectin from Sigma type IV S) dissolved in hexane (0.5%) was spread on the top of the electrolyte solution (1 M KCl/10 mM HEPES, pH 7.4) in both compartments of the measuring cell. Bilayer formation was achieved by lowering and raising the level up in one or both compartments and monitoring capacity responses. Voltage was applied through an Ag/AgCl electrode in the *cis* side and the *trans* side was grounded.

The purified EtpB proteins were added to the *cis* side (5–100 ng/ml). For the macroscopic conductance experiments, doped membranes were subjected to slow voltage ramps (10 mV/s), and the transmembrane currents were amplified (BBA-01; Eastern Scientific, Rockville, MD). The current–voltage curves were stored on a computer and analyzed with Scope software (Bio-Logic, Claix, France).

For single-channel recordings, currents were amplified and potentials were applied simultaneously by a BLM 120 amplifier (Bio-Logic). Single channel currents were monitored with an oscilloscope (TDS 3012, Tektronix, Beaverton, OR) and stored on a CD recorder via a DRA 200 interface (Bio-Logic) for off-line analysis. CD data were then analyzed by the WinEDR (Bio-Logic) and Clampfit (Molecular Devices, Sunnyvale, CA) softwares. Data were filtered at 1 kHz before digitizing at 11.2 kHz for analysis.

Protein Sequence Analysis

Protein sequences homologous to EtpB were identified in the GenBank, EMBL, and SwissProt databases by using the BLAST network service at the National Center for Biotechnology Information (Altschul et al. 1990). Results were confirmed by using the Protein Family Database Pfam at the Sanger Center (http://www.sanger.ac.uk/Software/Pfam/) (Bateman et al. 2002). Prediction of the secondary structural elements of EtpB was performed using the Psi-Pred (http://bioinf.cs.ucl.ac.uk/psipred/) software with the default parameters of the version 2.6.

Molecular Modeling of EtpB

Homology-based molecular modeling of EtpB was performed as follows. The EtpB sequence was aligned by CLUSTALW program (http://www.ebi.ac.uk/Tools/clustalw2) with several other homologous sequences including FhaC protein from *B. pertussis* of which a crystal structure has been already resolved (PDB code 2qdz) (Clantin et al. 2007). The crystal structure of FhaC was then used as an initial template for the modeling. The amino acid sequence of the template was edited in accordance with the EtpB sequence using the homology modeling option of Insight II program (Dayringer et al. 1986). Subsequently, some loops of the initial model were modeled manually. The structure was further refined by the energy minimization procedure that was based on the steepest descent algorithm implemented in the discovery subroutine of Insight II, and tethering heavy backbone atoms to their starting conformations with force constant $K = 100$. The next stage of minimization was 500 steps of the conjugate gradients algorithm, tethering the backbone atoms with lower force ($K = 50$), and then 300 steps with $K = 25$. The consistent valence force field and the distance dependent dielectric constant were used. Figure 4 was generated with Pymol (DeLano 2002).

Results and Discussion

Overexpression of the Recombinant EtpB in *E. coli* and Its Biochemical Characterization

EtpB was overproduced in an *E. coli* BL21(DE3)*omp8* strain. This strain is particularly useful for the production and subsequent characterization of heterologous OM proteins because it is devoid of numerous porins. This allows the analysis of expressed membrane proteins without contamination from endogenous *E. coli* porins (Prilipov et al. 1998). After IPTG induction of the recombinant gene, protein expression was analyzed by SDS-PAGE. Figure 1a shows a gel run with samples from the bacteria liquid culture before and after IPTG addition.

An N-proximal polyhistidine (His_6) tag was introduced into the EtpB coding sequence to facilitate purification of the protein. EtpB was extracted from membranes with OPOE detergent and subjected to a metal chelate affinity chromatography followed by a gel filtration chromatography in the continued presence of OPOE detergent (Fig. 1b, lanes 1 and 2). Protein bands with an apparent molecular mass of approximately 65 kDa (corresponding to the presumed MW of EtpB) were excised from the gel and analyzed by mass spectrometry. This revealed proper cleavage of the OmpA signal peptide and generation of the mature His tagged EtpB protein (data not shown). The EtpB proteins were treated with thrombin to remove the His_6 tag. Multiple conditions for thrombin cleavage (including during the chelate affinity chromatography or on the EtpB purified fractions in solution), were attempted but we were unable to remove the tag. This suggests that EtpB was

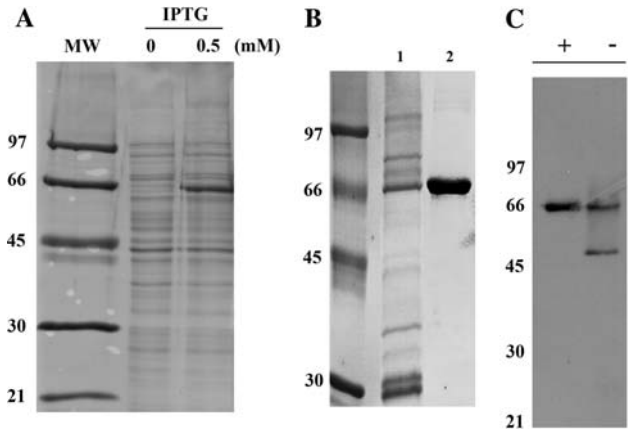

Fig. 1 Overexpression, purification, and folding of the recombinant EtpB proteins. **a** Analysis of the overexpression of recombinant His_6-EtpB by 12% SDS-PAGE after Coomassie blue staining. A total of 1 ml of liquid culture was removed before (*left lane* 20 µl loaded) or after (*middle lane* 20 µl loaded) the addition of a final concentration of 0.5 mM IPTG. Each sample was incubated for 3 h at 37°C. The bands of the right lane indicate the sizes of the molecular mass markers (MW). **b** Coomassie blue–stained gel of eluted fractions of purified recombinant His_6-EtpB after a metal chelate affinity chromatography (*lane 1*) followed by gel filtration chromatography (*lane 2*). The molecular mass markers (MW) for 97, 66, 45, 30, and 21 kDa are shown. **c** Western blot analyses using anti-EtpB polyclonal antibodies of the eluted fractions of purified His_6-EtpB after gel filtration chromatography. The eluted fractions were heated for 10 min at 95°C (+) or not (−) in semidenaturated conditions (10% PAGE at 4°C, 0.1% SDS final in both Laemmli and electrophoresis buffers). The molecular mass markers (in kDa) are indicated

folded in a conformation in which the cleavage site was inaccessible to thrombin, similar to the inaccessibility of thrombin cleavage sites previously reported for other OM proteins (Siroy et al. 2005).

OM proteins with β-barrel structures exhibit heat-modifiable electrophoretic mobility behavior. For example, the folded and compact β-barrel conformations migrate more quickly in SDS-PAGE than their denatured forms (Hancock and Carey 1979; Schnaitman 1973). We next determined the correct folding of the purified EtpB proteins by examining these heat-modifiability properties. Nonheated purified EtpB proteins subjected to electrophoresis under semidenaturing conditions (0.1% SDS final in both Laemmli and electrophoresis buffers) at 4°C appeared to migrate faster than the heated denatured monomer. This suggests a folded monomer conformation. The identity of these proteins was further confirmed by western blot analysis using anti-EtpB polyclonal antibodies (Fig. 1c). Taken together, these data are consistent with the idea that EtpB is an OM protein arranged into β-barrel. This is an architecture that EtpB shares with other previously characterized TpsB proteins (Jacob-Dubuisson et al. 1999; Li et al. 2007).

Functional Characterization of WT EtpB in Artificial Lipid Bilayers

It is known that the β-barrels of TpsB OM proteins are able to form ion-conductive pores (Duret et al. 2008; Konninger et al. 1999; Meli et al. 2006). We assessed pore-forming activity of EtpB in planar lipid bilayers to confirm our hypothesis that EtpB forms an ion-conducting pore (Fig. 2). Ion channel properties of EtpB were first examined by recording macroscopic current–voltage (I/V) curves (Fig. 2a). Up to a hundred channels are incorporated in this configuration and submitted to slow voltage ramps at relatively high protein concentrations. Macroscopic *I/V* curves are useful to screen the functional properties of potential channel-forming molecules in lipid bilayers.

The *I/V* curves obtained after addition of EtpB at a final concentration of approximately 100 ng/ml to the *cis* side of azolectin bilayers revealed a nonlinear current/voltage relationship. The *I/V* curve also indicated a slight asymmetric behavior as demonstrated by the unequal currents observed between the positive and the negative quadrants. For example, a maximum current amplitude of $\sim$5 nA is revealed at +80 mV while the I/V curve exhibits a lower current of $\sim$3 nA at −80 mV. This result indicates that functionally asymmetric EtpB molecules insert in a preferred orientation into lipid bilayers. The absolute orientation of the molecules could not, however, be determined from these current–voltage recordings. Such polarity-dependent behavior has been observed with other β-barrel proteins (Danelon et al. 2003; Hinnah et al. 1997; Surrey and Jahnig 1992) and with well characterized TpsB proteins such as FhaC of *B. pertussis* and HMW1B of *H. influenzae*. In the case of FhaC, the macroscopic *I/V* current showed an asymmetric behavior and an activation of the channel generating a hysteresis at potentials more negative than −60 mV. In the case of HMW1B, a greatly increased activity occurred at potentials larger than ±100 mV (Duret et al. 2008; Meli et al. 2006).

We further examined the influence of membrane potential on conductance in single-channel experiments in order to study the pore characteristics of EtpB in further detail and to confirm the asymmetric properties in ion conduction observed from the macroscopic *I/V* curves. To this end, very small amounts of EtpB molecules were introduced into the *cis* compartment, bathing the lipid bilayer (final concentration of approximately 0.1 to 1 ng/ml). Figure 2b shows ionic current recordings from single-channel experiments at different membrane potentials. The current increased with increasing voltages between ±60 and ±120 mV. EtpB displayed frequent, transient transitions to various open levels at all holding voltages. The measurements of the openings were still reliable at ±120 mV and three types of openings could be clearly

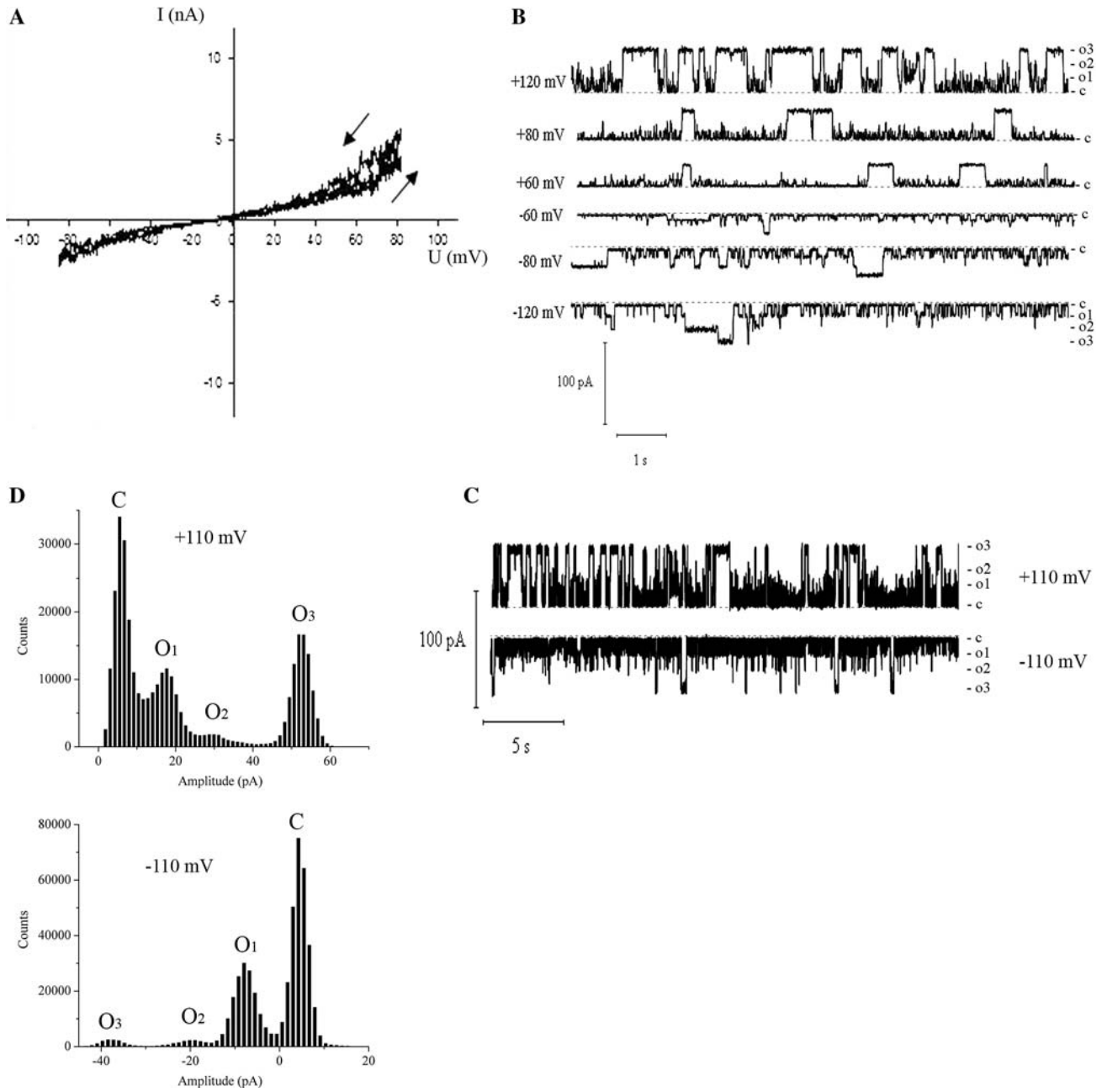

Fig. 2 Channel activity of the recombinant EtpB proteins. **a** Multi-channel I/V curves of EtpB obtained between −80 and +80 mV. Measurements were performed in 1 M KCl, 10 mM HEPES (pH 7.4). The arrows indicate the direction of the applied voltage ramp ($n = 4$). **b** Single-channel recordings of EtpB obtained from the same single inserted protein at the indicated voltages ($n = 4$). **c** Selected recordings showing the subconductance levels of the EtpB single-channel at ±110 mV. *O*, open state at different current levels; *C*, closed state. Measurements were performed in 0.5 M KCl, 10 mM HEPES (pH 7.4). **d** Corresponding amplitude histogram of the entire single-channel recordings at ±110 mV. The dashed lines represent the zero current level. All experiments were performed at room temperature (23°C)

defined. Openings of small conductance (O_1) and medium conductance (O_2) with a current of ∼20 and 45 pA, respectively, and openings of larger conductance (O_3) with a current of ∼75 pA at +120 mV in 0.5 M KCl (Fig. 2b) were all observed. The opening kinetics were variable and the channel fluctuated between these three conductance states at all holding voltages. The channel exhibited a moderate probability of being in the maximal open state. Po was ∼0.20 and ∼0.12 at +80 and −80 mV, whereas Po was ∼0.53 and ∼0.39 at +110 mV and −110 mV. Interestingly, we observed that the channel reached openings of larger conductance (O_3) more frequently at positive

holding voltages than at negative holding voltages because the Po of O_3 in the entire illustrated trace was ~0.27 and ~0.035 at +110 mV and −110 mV (Fig. 2c). This behavior, dependent on the polarity of the voltage, is in agreement with the asymmetric macroscopic current–voltage curves we initially recorded. These characteristics strongly suggest that EtpB is a functionally asymmetric protein that inserts preferentially in the membrane.

The amplitude histograms obtained from recordings at ±110 mV displayed three peaks corresponding to the main states that the EtpB channel exhibited (Fig. 2d). The peak corresponding to the higher open state at +110 mV (i.e., O_3) has the highest amplitude of the three open states indicating that EtpB spends a majority of time in that open conformation. The conductance of this main opening O_3 (ΔG_3) was ~400 pS while ~250 and ~100 pS were estimated for ΔG_2 and ΔG_1, corresponding to the medium (O_2) and small (O_1) openings, respectively. The majority of the experiments were performed in 0.5 M KCl but similar subconductance states were also observed at lower and higher salt concentrations (data not shown).

The conductance values we observed for EtpB are in the same order of magnitude as those reported for other TpsB proteins such as FhaC, ShlB and HMW1B (Duret et al. 2008; Jacob-Dubuisson et al. 1999; Konninger et al. 1999; Meli et al. 2006). In agreement with previous results, channels with heterogeneous conductance values have also been described for some of these other TpsB proteins. Closer inspection of the current traces of both FhaC and HMW1B revealed that the channels made direct transitions between the closed state and the largest amplitude, as well as direct transitions between subconductance states (Duret et al. 2008; Jacob-Dubuisson et al. 1999; Meli et al. 2006). The channel properties of the chloroplast protein import channel Toc75, a protein belonging to the Omp85/TpsB superfamily, also revealed the presence of a main level of conductance accompanied of two substates (Hinnah et al. 1997).

The main conductance state of EtpB channel (ΔG_3, ~400 pS) was almost twice as large as the medium conductance state (ΔG_2, ~250 pS) and four times as large as the smallest conductance state (ΔG_1, ~100 pS). Two different interpretations can explain this behavior. EtpB could insert as a monomer and first partially open into two substates before opening fully (i.e., O_3). Alternatively, EtpB might not be active as a monomer in this assay. Rather, oligomers may need to form in the bilayer membrane. In this case our results would indicate that one EtpB monomeric channel is mostly open, while another opens and closes more frequently. Previous data strongly argued that monomeric FhaC and ShlB form the functional transport unit (Jacob-Dubuisson et al. 1999; Konninger et al. 1999; Meli et al. 2006). Moreover, FhaC was crystallized as a monomer, suggesting that it is also predominantly monomeric in membranes in vivo (Clantin et al. 2007). In contrast, the HMW1B transporter has been reported to form oligomers but the size of the complexes are still under debate. HMW1B was first described as a tetramer (Surana et al. 2004), but it was later found to form dimers with a twin pore structure (Li et al. 2007). Recently, Duret et al. (2008) showed that the HMW1B channel kinetic behavior is characterized by the presence of two well defined conductance states but these authors could not confirm that these properties are related to the oligomeric nature of the channel.

In summary, the analysis of the channel-forming properties of recombinant EtpB suggest that the EtpB protein forms channels with a preferential orientation in bilayer membranes, similar to prior observations for other β-barrel proteins. Moreover, EtpB clearly fluctuates between several well-defined conductance states. Our results support the existence of a β-barrel channel in EtpB through which EtpA might be exported, although the channel characteristics did not allow us to discriminate between a monomeric or oligomeric nature of EtpB channels.

Sequence Analysis and Molecular Modeling of EtpB

EtpB (accession number AY920525) is predicted to be a 603 aa protein with an estimated molecular mass of 64.3 kDa according to Swiss-Prot search. BLAST search (http://blast.ncbi.nlm.nih.gov/Blast.cgi) against sequences of PDB database yields a significant match (E-value = $7*e^{-4}$ and 20% of identity, 35% of similarity) between EtpB and the membrane protein FhaC which has a known 3D structure (PDB-code 2qdz) (Clantin et al. 2007). In addition, comparison of EtpB and FhaC sequences with Psi-Pred (http://bioinf.cs.ucl.ac.uk/psipred/) and the PFAM/SANGER data bank (http://www.sanger.ac.uk/Software/Pfam/) programs also pointed out conservation of secondary structural elements characteristic of FhaC along the entire EtpB sequence (Fig. 3). Indeed, an N-terminal helix, equivalent to the H1 helix in FhaC structure, two POTRA domains and 16 successive β-strands were predicted in EtpB, suggesting a similar overall fold for both proteins. EtpB is homologous to another well-studied TpsB protein HMW1B from *H. influenzae* (E-value = $7*e^{-6}$ and 19% of identity, 36% of similarity) (Fig. 3). However, the sequence of HMW1B seems to start with the two POTRA domains after the signal peptide, indicating that the H1 helix equivalent element is missing in HMW1B. EtpB sequence also exhibits other common features typically described for bacteria OM proteins, including a consensus sequence at the C-terminus, consisting of a C-terminal phenylalanine preceded at every second position by four nonpolar amino acids (Struyve et al. 1991).

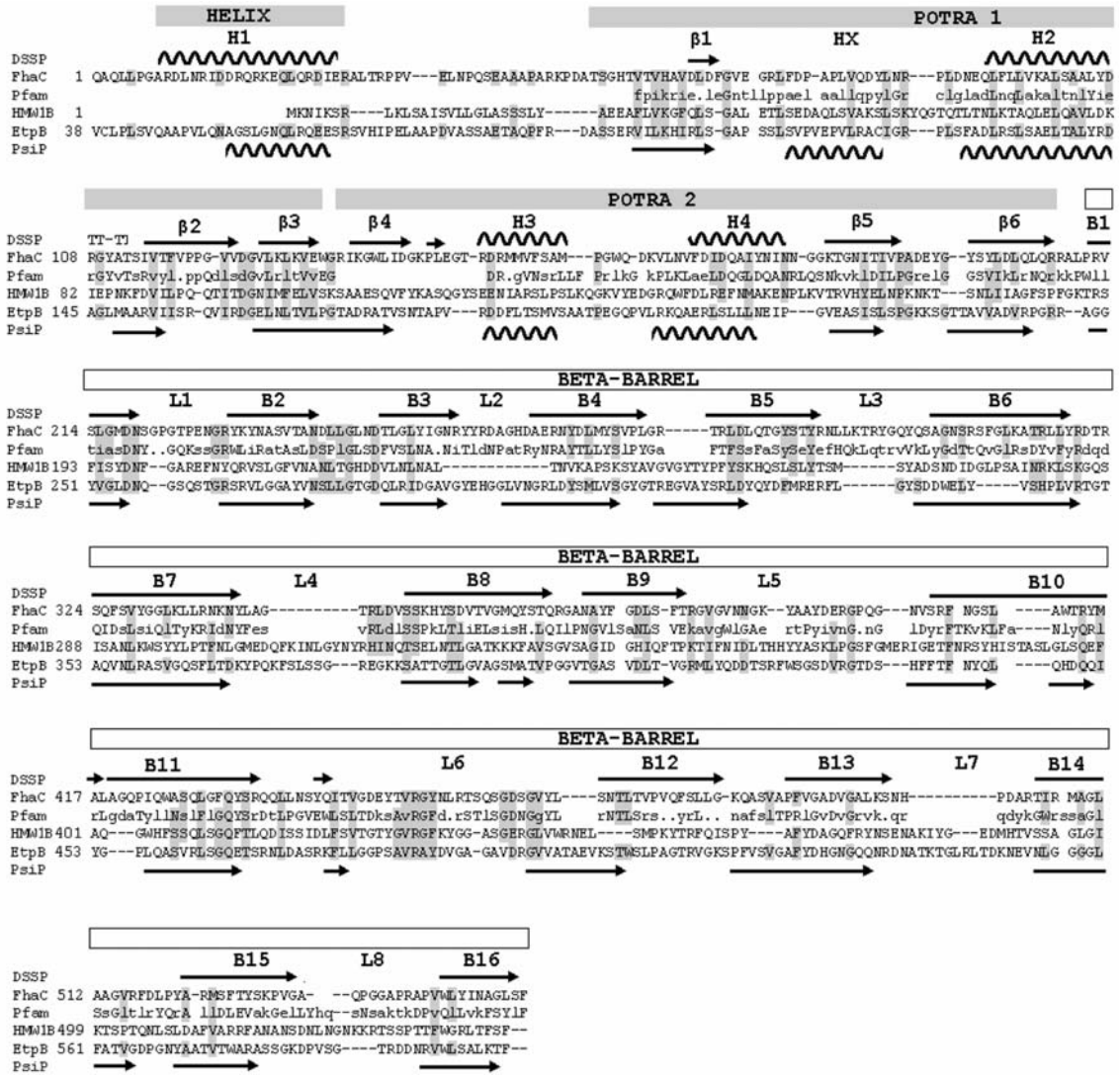

Fig. 3 Sequence alignment of FhaC and EtpB proteins used for molecular modeling. The first line shows secondary structure of FhaC (using define secondary structure of proteins criteria). The second, fourth, and fifth lines are amino acid sequences of FhaC, HMW1B, and EtpB, respectively. Only the HMW1B sequence starts with its signal peptide. The third line represents a consensus sequence of POTRA 1 and the remaining portion of the protein taken from PFAM database (accession numbers PF08479 and PF03865). The sixth line corresponds to a predicted secondary structure of EtpB which was obtained by using the Psi-Pred (http://bioinf.cs.ucl.ac.uk/psipred/) software with the default parameters (version 2.6). Identical and similar amino acids in both proteins are colored in *grey*. Elements of β-structure and α-helices are shown by *arrows* and *waved lines*

Homology-based molecular modeling supported the conclusions of our sequence analysis. The similarity between FhaC and EtpB sequences is relatively low (approximately 20% identities) but the availability of the 3D structure for FhaC and the generation of the multiple sequence alignments allow us to validate the alignment used for the homology modeling (Fig. 3). The alignment was obtained by BLAST and subsequently verified by generation of multiple sequence alignments with several homologous proteins by CLUSTALW (http://www.ebi.ac.uk/Tools/clustalw2). Because of the lack of significant sequence similarities, the alignments of some loop regions were corrected manually by using structural information such as correlation between known and predicted secondary structures and correspondence between the highly conserved positions in the amino acid sequence alignment and residues forming the hydrophobic core in the 3D structure of proteins. The molecular model of EtpB is shown in Fig. 4.

The EtpB model and FhaC structure have very similar overall 3D structures, but our modeling revealed some small differences. For example, while periplasmic POTRA domains are found in EtpB and FhaC, the crosslink between POTRA 2 domain and β-barrel of EtpB is shorter

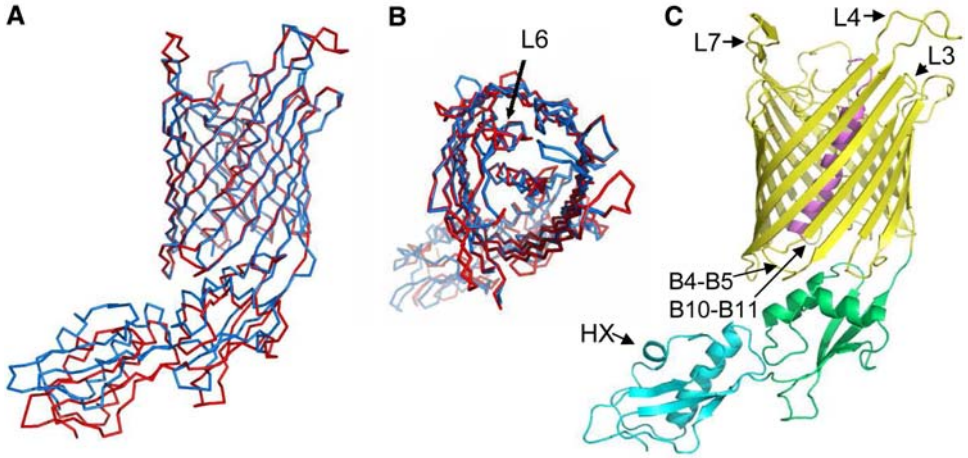

Fig. 4 Structural model of EtpB. **a, b** Superposition of the crystal structure of FhaC (*blue*) and EtpB model (*red*). **c** Ribbon representation of EtpB model. The N-terminal alpha helix is in magenta, POTRA 1 and 2 domains in *green* and *light blue*. The β-barrel is in *yellow*. Loops of EtpB that are different from FhaC loops are labeled. B4-B5 and B10-B11 indicate loops between corresponding β-strands (Color figure online)

than in FhaC. This suggests a slightly different orientation of POTRA domains relative to the β-barrels in EtpB and FhaC. Moreover, the POTRA 1 domain of EtpB has a short α-helix (HX) in the region P113-C121, in contrast to FhaC domain, which does not contain an α-helix in this region. The POTRA 2 domains of EtpB and FhaC, despite their low sequence identity, do have a similar basic 3D structure composed of a three-stranded β sheet overlaid with a pair of α-helices arranged in the order of β-α-α-β-β. This structural element is also conserved in the five POTRA domains of YaeT of *E coli*, a prototypic Omp85 protein involved in the assembly of OM proteins (Kim et al. 2007; Knowles et al. 2008). POTRA domains have been proposed to bind nascent folding substrates in vivo (Clantin et al. 2007). Recently Knowles et al. (2008) demonstrated by NMR titration measurements that POTRA domains of YaeT were able to interact with peptides mimicking nascent unfolded OM proteins. The presence of two POTRA domains in EtpB protein suggests that the binding of the unfolded EtpA adhesin in the periplasm could occur utilizing a similar mechanism.

In our EtpB model, we observed that the C-terminal part of the protein was well superimposed on the C-terminal structure of FhaC, suggesting that the β-barrel of EtpB could also be composed of 16 transmembrane β strands. This common architecture suggests that EtpB and FhaC would have similar pore dimensions. The mean deviations observed for the EtpB backbone as compared with FhaC structure in the β-barrel domain are located in extracellular and periplasmic loops connecting the transmembrane strands. Thus, an outside EtpB loop L3 is shorter than in FhaC, and loops L4 and L7 are longer (Fig. 4B). The periplasmic loop between B10 and B11 is shorter, while the loop between B4 and B5 is longer than in FhaC. Similar to the FhaC structure, the L6 loop of EtpB is inside the pore occupying the same position (Fig. 4C), but this loop is slightly longer in EtpB than in FhaC (Fig. 3). The L6 loop of FhaC has been shown to be essential in the secretion mechanism because deletion of the large L6 loop abolished adhesin secretion (Clantin et al. 2007). This loop also undergoes a conformational change during secretion (Guedin et al. 2000). It seems reasonable that the L6 loop plugging the pore of EtpB would also be strongly involved in the secretion of its TpsA partner.

Despite the fact that the main function of the TpsB transporters is devoted to the secretion of TpsA exoproteins, it is also known that some TpsB proteins are involved in additional functions by activating or modifying their partner proteins (Choi et al. 2007; Hertle et al. 1997; Ondraczek et al. 1992; Walker et al. 2004). Because of its considerable homology with the OM adhesin Enf of enteroaggregative *E. coli*, it was suggested that EtpB might have a second function as an adhesin. Moreover, a previous study has revealed that a laboratory strain of *E. coli* (Novablue) expressing the recombinant EtpB improved its adherence to Caco-2 cells compared with the control strain in vitro (Fleckenstein et al. 2006). Therefore, the differences we have observed in the loops, particularly in the extracellular loops, may be responsible for specific regulation of this EtpB adhesin function. These structural characteristics can account for the small differences we observed in the channel behavior of the EtpB and FhaC. The EtpB model revealed that, similar to FhaC, an N-terminal α-helix could be located inside the pore. Curiously, this α-helix merging into the aqueous pore is more hydrophobic in EtpB than in FhaC (Fig. 3). Deletion of this so-called H1 helix in FhaC did not affect FHA secretion ruling out an essential contribution of this structural element in the secretion mechanism.

Recent structural studies of another TpsB member, HMW1B from *H. influenzae,* that shows sequence similarities with EtpB (Fig. 3), revealed the formation of a dimeric complex including a twin pore in the presence of lipids (Li et al. 2007). Such dimeric structures were also

observed for other protein translocating channels like the TIM and TOM complexes responsible for transport of nuclear-encoded preproteins into mitochondrial membranes and the PapC and FimD OM usher involved in the assembly of the *E. coli* P and type 1 pili, respectively (Li et al. 2004; Rehling et al. 2003; Remaut et al. 2008). The presence of twin-pore machinery has not been documented in FhaC and EtpB studies. It is conceivable, however, that these proteins might form oligomers in vivo because large FhaC complexes have been detected in *B. pertussis* membranes (Jacob-Dubuisson et al. 1999).

In conclusion, we have established that EtpB is a heat-modifiable OM protein that is able to form pores in planar lipid bilayer membranes. EtpB electrophysiological properties suggest a structural asymmetry similar to those observed for some other TpsB members, which are mainly folded in a β-barrel. Molecular EtpB modeling based on the recently solved FhaC X-ray structure further supports the idea that EtpB is a TpsB protein. The EtpB transporter is predicted to comprise a 16-stranded β-barrel that is occluded by an N-terminal α-helix and an extracellular loop. Interestingly, as is known for other TpsB members, EtpB might also contain 2 periplasmic POTRA domains likely involved in the translocation of EtpA through the OM. Although the EtpB model is very similar to the structure of FhaC, some different structural elements are present in the EtpB protein: (i) the existence of longer or shorter extracellular and periplasmic loops connecting the β-strands, (ii) different orientation of the POTRA domains relative to the β-barrel. These structural particularities might be involved in specific interactions between EtpB and its TpsA partner as well as in the reported adhesin function of EtpB.

Thus, the molecular EtpB modeling presented here provides the foundation for rational mutagenesis studies to go further in deciphering the EtpB structure. For instance, gene fusions to alkaline phosphatase or other epitope fusions could be used to confirm the accessibility of putative exposed loops to the surface. Moreover, the role of nonconserved regions of EtpB could be further examined by looking at the channel properties and by quantifying the EtpA secretion activity of some EtpB mutants.

Taken together, our data may help in elucidating the structure-function relationship of the OM EtpB transporter involved in the TPS pathway of ETEC. From a clinical point of view, a better knowledge of the TPS pathway of ETEC may provide new targets for vaccine development.

Acknowledgments We thank Gerard Molle for his interest in this work, and Francoise Jacob-Dubuisson and Gilles Labesse for helpful discussions. We thank James M. Fleckenstein for the gift of the EtpB plasmid and EtpB antibodies. Albano C. Meli is the recipient of a predoctoral fellowship from the Ministère de l'Education Nationale, de la Recherche et de la Technologie (grant ACI BCMS 2004).

References

Altschul SF, Gish W, Miller W, Myers EW, Lipman DJ (1990) Basic local alignment search tool. J Mol Biol 215:403–410

Barenkamp SJ, St Geme JWIII (1994) Genes encoding high-molecular-weight adhesion proteins of nontypeable *Haemophilus influenzae* are part of gene clusters. Infect Immun 62:3320–3328

Bateman A, Birney E, Cerruti L, Durbin R, Etwiller L, Eddy SR, Griffiths-Jones S, Howe KL, Marshall M, Sonnhammer EL (2002) The Pfam protein families database. Nucleic Acids Res 30:276–280

Beatty ME, Bopp CA, Wells JG, Greene KD, Puhr ND, Mintz ED (2004) Enterotoxin-producing *Escherichia coli* O169:H41, United States. Emerg Infect Dis 10:518–521

Beatty ME, Adcock PM, Smith SW, Quinlan K, Kamimoto LA, Rowe SY, Scott K, Conover C, Varchmin T, Bopp CA, Greene KD, Bibb B, Slutsker L, Mintz ED (2006) Epidemic diarrhea due to enterotoxigenic *Escherichia coli*. Clin Infect Dis 42:329–334

Cascales E, Christie PJ (2003) The versatile bacterial type IV secretion systems. Nat Rev Microbiol 1:137–149

Choi PS, Dawson AJ, Bernstein HD (2007) Characterization of a novel two-partner secretion system in *Escherichia coli* O157:H7. J Bacteriol 189:3452–3461

Clantin B, Hodak H, Willery E, Locht C, Jacob-Dubuisson F, Villeret V (2004) The crystal structure of filamentous hemagglutinin secretion domain and its implications for the two-partner secretion pathway. Proc Natl Acad Sci USA 101:6194–6199

Clantin B, Delattre AS, Rucktooa P, Saint N, Meli AC, Locht C, Jacob-Dubuisson F, Villeret V (2007) Structure of the membrane protein FhaC: a member of the Omp85-TpsB transporter superfamily. Science 317:957–961

Danelon C, Brando T, Winterhalter M (2003) Probing the orientation of reconstituted maltoporin channels at the single-protein level. J Biol Chem 278:35542–35551

Daniels NA (2006) Enterotoxigenic *Escherichia coli*: traveler's diarrhea comes home. Clin Infect Dis 42:335–336

Dayringer HE, Tramontano A, Sprang SR, Fletterick RJ (1986) Interactive program for visualization and modelling of proteins, nucleic acids and small molecules. J Mol Graph 4:82–87

DeLano WL (2002) The PyMol molecular graphics system. DeLano Scientific, San Carlos, CA

Desvaux M, Parham NJ, Henderson IR (2004) Type V protein secretion: simplicity gone awry? Curr Issues Mol Biol 6:111–124

Duret G, Szymanski M, Choi KJ, Yeo HJ, Delcour AH (2008) The TpsB translocator HMW1B of *Haemophilus influenzae* forms a large conductance channel. J Biol Chem 283:15771–15778

Fleckenstein JM, Roy K, Fischer JF, Burkitt M (2006) Identification of a two-partner secretion locus of enterotoxigenic *Escherichia coli*. Infect Immun 74:2245–2258

Guedin S, Willery E, Tommassen J, Fort E, Drobecq H, Locht C, Jacob-Dubuisson F (2000) Novel topological features of FhaC, the outer membrane transporter involved in the secretion of the *Bordetella pertussis* filamentous hemagglutinin. J Biol Chem 275:30202–30210

Hancock RE, Carey AM (1979) Outer membrane of *Pseudomonas aeruginosa*: heat-2-mercaptoethanol-modifiable proteins. J Bacteriol 140:902–910

Henderson IR, Navarro-Garcia F, Nataro JP (1998) The great escape: structure and function of the autotransporter proteins. Trends Microbiol 6:370–378

Hertle R, Brutsche S, Groeger W, Hobbie S, Koch W, Konninger U, Braun V (1997) Specific phosphatidylethanolamine dependence of *Serratia marcescens* cytotoxin activity. Mol Microbiol 26:853–865

Hinnah SC, Hill K, Wagner R, Schlicher T, Soll J (1997) Reconstitution of a chloroplast protein import channel. EMBO J 16:7351–7360

Holland IB (2004) Translocation of bacterial proteins—an overview. Biochim Biophys Acta 1694:5–16

Jacob-Dubuisson F, El-Hamel C, Saint N, Guedin S, Willery E, Molle G, Locht C (1999) Channel formation by FhaC, the outer membrane protein involved in the secretion of the *Bordetella pertussis* filamentous hemagglutinin. J Biol Chem 274:37731–37735

Jacob-Dubuisson F, Locht C, Antoine R (2001) Two-partner secretion in gram-negative bacteria: a thrifty, specific pathway for large virulence proteins. Mol Microbiol 40:306–313

Jacob-Dubuisson F, Villeret V, Clantin B, Delattre AS, Saint N (2009) First structural insights into the TpsB/Omp85 superfamily. Biol Chem 390(8):675–684

Junker M, Schuster CC, McDonnell AV, Sorg KA, Finn MC, Berger B, Clark PL (2006) Pertactin beta-helix folding mechanism suggests common themes for the secretion and folding of autotransporter proteins. Proc Natl Acad Sci USA 103:4918–4923

Kajava AV, Steven AC (2006) The turn of the screw: variations of the abundant beta-solenoid motif in passenger domains of Type V secretory proteins. J Struct Biol 155:306–315

Kajava AV, Cheng N, Cleaver R, Kessel M, Simon MN, Willery E, Jacob-Dubuisson F, Locht C, Steven AC (2001) Beta-helix model for the filamentous haemagglutinin adhesin of *Bordetella pertussis* and related bacterial secretory proteins. Mol Microbiol 42:279–292

Kim S, Malinverni JC, Sliz P, Silhavy TJ, Harrison SC, Kahne D (2007) Structure and function of an essential component of the outer membrane protein assembly machine. Science 317:961–964

Knowles TJ, Jeeves M, Bobat S, Dancea F, McClelland D, Palmer T, Overduin M, Henderson IR (2008) Fold and function of polypeptide transport-associated domains responsible for delivering unfolded proteins to membranes. Mol Microbiol 68:1216–1227

Knowles TJ, Scott-Tucker A, Overduin M, Henderson IR (2009) Membrane protein architects: the role of the BAM complex in outer membrane protein assembly. Nat Rev Microbiol 7:206–214

Konninger UW, Hobbie S, Benz R, Braun V (1999) The haemolysin-secreting ShlB protein of the outer membrane of *Serratia marcescens*: determination of surface-exposed residues and formation of ion-permeable pores by ShlB mutants in artificial lipid bilayer membranes. Mol Microbiol 32:1212–1225

Kostakioti M, Newman CL, Thanassi DG, Stathopoulos C (2005) Mechanisms of protein export across the bacterial outer membrane. J Bacteriol 187:4306–4314

Li H, Qian L, Chen Z, Thibault D, Liu G, Liu T, Thanassi DG (2004) The outer membrane usher forms a twin-pore secretion complex. J Mol Biol 344:1397–1407

Li H, Grass S, Wang T, Liu T, St Geme JWIII (2007) Structure of the *Haemophilus influenzae* HMW1B translocator protein: evidence for a twin pore. J Bacteriol 189:7497–7502

Meli AC, Hodak H, Clantin B, Locht C, Molle G, Jacob-Dubuisson F, Saint N (2006) Channel properties of TpsB transporter FhaC point to two functional domains with a C-terminal protein-conducting pore. J Biol Chem 281:158–166

Mota LJ, Sorg I, Cornelis GR (2005) Type III secretion: the bacteria-eukaryotic cell express. FEMS Microbiol Lett 252:1–10

Mougous JD, Gifford CA, Ramsdell TL, Mekalanos JJ (2007) Threonine phosphorylation post-translationally regulates protein secretion in *Pseudomonas aeruginosa*. Nat Cell Biol 9:797–803

Nelson KM, Young GM, Miller VL (2001) Identification of a locus involved in systemic dissemination of *Yersinia enterocolitica*. Infect Immun 69:6201–6208

Ondraczek R, Hobbie S, Braun V (1992) In vitro activation of the *Serratia marcescens* hemolysin through modification and complementation. J Bacteriol 174:5086–5094

Prilipov A, Phale PS, Van Gelder P, Rosenbusch JP, Koebnik R (1998) Coupling site-directed mutagenesis with high-level expression: large scale production of mutant porins from *E. coli*. FEMS Microbiol Lett 163:65–72

Pukatzki S, Ma AT, Sturtevant D, Krastins B, Sarracino D, Nelson WC, Heidelberg JF, Mekalanos JJ (2006) Identification of a conserved bacterial protein secretion system in *Vibrio cholerae* using the *Dictyostelium* host model system. Proc Natl Acad Sci USA 103:1528–1533

Rehling P, Model K, Brandner K, Kovermann P, Sickmann A, Meyer HE, Kuhlbrandt W, Wagner R, Truscott KN, Pfanner N (2003) Protein insertion into the mitochondrial inner membrane by a twin-pore translocase. Science 299:1747–17451

Remaut H, Tang C, Henderson NS, Pinkner JS, Wang T, Hultgren SJ, Thanassi DG, Waksman G, Li H (2008) Fiber formation across the bacterial outer membrane by the chaperone/usher pathway. Cell 133:640–652

Roels TH, Proctor ME, Robinson LC, Hulbert K, Bopp CA, Davis JP (1998) Clinical features of infections due to *Escherichia coli* producing heat-stable toxin during an outbreak in Wisconsin: a rarely suspected cause of diarrhea in the United States. Clin Infect Dis 26:898–902

Roy K, Hamilton D, Allen KP, Randolph MP, Fleckenstein JM (2008) The EtpA exoprotein of enterotoxigenic *Escherichia coli* promotes intestinal colonization and is a protective antigen in an experimental model of murine infection. Infect Immun 76:2106–2112

Roy K, Hilliard GM, Hamilton DJ, Luo J, Ostmann MM, Fleckenstein JM (2009) Enterotoxigenic *Escherichia coli* EtpA mediates adhesion between flagella and host cells. Nature 457:594–598

Sanchez-Pulido L, Devos D, Genevrois S, Vicente M, Valencia A (2003) POTRA: a conserved domain in the FtsQ family and a class of beta-barrel outer membrane proteins. Trends Biochem Sci 28:523–526

Schell MA, Ulrich RL, Ribot WJ, Brueggemann EE, Hines HB, Chen D, Lipscomb L, Kim HS, Mrazek J, Nierman WC, Deshazer D (2007) Type VI secretion is a major virulence determinant in *Burkholderia mallei*. Mol Microbiol 64:1466–1485

Schnaitman CA (1973) Outer membrane proteins of *Escherichia coli.* I. Effect of preparative conditions on the migration of protein in polyacrylamide gels. Arch Biochem Biophys 157:541–552

Siroy A, Molle V, Lemaitre-Guillier C, Vallenet D, Pestel-Caron M, Cozzone AJ, Jouenne T, De E (2005) Channel formation by CarO, the carbapenem resistance–associated outer membrane protein of *Acinetobacter baumannii*. Antimicrob Agents Chemother 49:4876–4883

St Geme JWIII, Grass S (1998) Secretion of the *Haemophilus influenzae* HMW1 and HMW2 adhesins involves a periplasmic intermediate and requires the HMWB and HMWC proteins. Mol Microbiol 27:617–630

Struyve M, Moons M, Tommassen J (1991) Carboxy-terminal phenylalanine is essential for the correct assembly of a bacterial outer membrane protein. J Mol Biol 218:141–148

Surana NK, Grass S, Hardy GG, Li H, Thanassi DG, Geme JWIII (2004) Evidence for conservation of architecture and physical properties of Omp85-like proteins throughout evolution. Proc Natl Acad Sci USA 101:14497–14502

Surrey T, Jahnig F (1992) Refolding and oriented insertion of a membrane protein into a lipid bilayer. Proc Natl Acad Sci USA 89:7457–7461

Thanassi DG, Stathopoulos C, Karkal A, Li H (2005) Protein secretion in the absence of ATP: the autotransporter, two-partner

secretion and chaperone/usher pathways of gram-negative bacteria (review). Mol Membr Biol 22:63–72

Walker G, Hertle R, Braun V (2004) Activation of *Serratia marcescens* hemolysin through a conformational change. Infect Immun 72:611–614

Yen MR, Peabody CR, Partovi SM, Zhai Y, Tseng YH, Saier MH (2002) Protein-translocating outer membrane porins of gram-negative bacteria. Biochim Biophys Acta 1562:6–31

Yeo HJ, Yokoyama T, Walkiewicz K, Kim Y, Grass S, Geme JWIII (2007) The structure of the *Haemophilus influenzae* HMW1 propiece reveals a structural domain essential for bacterial two-partner secretion. J Biol Chem 282:31076–31084